NUMERICAL MODELLING OF CARRYOVER DEPOSITION IN KRAFT RECOVERY BOILERS

M. Bussmann[1], J. Mostaghimi[1], S. Chandra[1], H.N. Tran[2]
[1]Department of Mechanical and Industrial Engineering
[2]Department of Chemical Engineering and Applied Chemistry
Pulp and Paper Centre
University of Toronto
Toronto, Ontario, CANADA

ABSTRACT

The deposition of carryover, or molten and partially molten smelt and black liquor particles, is a primary source of plugging of flue gas passages within kraft recovery boilers. An improved understanding of how an individual particle impacts onto a heat transfer surface may result in strategies for reducing the deposition rate. A numerical model has been developed to simulate molten carryover droplet impact, to assess the influence of particle size, velocity and particle fluid properties on the consequent impact dynamics. Results of parametric studies using the model show that the liquid surface tension and the wetting behaviour of the liquid on the surface strongly affect the impact of small particles (diameter < 0.5 mm). Small particles are shown to spread uniformly and without disruption, and are likely to stick on impact. As the particle size and impact velocity increase, inertial effects become more significant. Particles larger than 1 mm will tend to splash on impact, forming small satellite particles which do not stick, and which may account for the presence of the small carryover particles found in precipitator dust.

INTRODUCTION

A primary cause of plugging of flue gas passages within kraft recovery boilers is the deposition of flow-entrained carryover particles onto heat transfer surfaces, particularly within the superheater region and at the boiler bank inlet. In effect, the tubes act as an unintentional filter, removing molten and partially molten particles which impact onto the tubes, spread, stick and solidify. The agglomeration of many such particles yields a carryover deposit.

Mass carryover deposition drastically reduces heat transfer efficiency and may lead to an unscheduled shut-down of a boiler due to plugging. Thus, an understanding of deposit growth is important, as it may lead to strategies to reduce the deposition rate and/or the cost of deposit removal. The overall goal of this research is to understand the relationship between boiler operating conditions and deposit growth, in order to predict and influence deposit properties and growth rate.

One key step towards this goal is to characterize the impact of a single carryover particle, whether onto a clean heat transfer tube or onto an existing deposit. Of interest is the influence of particle size, velocity and composition on the likelihood, for example, that a particle will stick to a surface rather than bounce off, or remain intact rather than break up. This paper presents results of a numerical model developed to simulate the impact of a fluid particle onto a solid surface. A problem definition and a description of the model are followed by results of a validation study to demonstrate the applicability of the model. Results are then presented of the influence of particle size, velocity, and fluid properties on carryover particle impact.

PROBLEM DEFINITION AND MODEL DESCRIPTION

Carryover particles originate as black liquor droplets sprayed into the lower section of a recovery boiler. While most droplets fall onto the char bed, some become entrained by the upward gas flow. The droplets burn during flight until they impact onto heat transfer tubes. At impact, the molten or partially molten particles are composed of Na_2CO_3 and Na_2SO_4, and may contain unburned carbon.

The objective of this study was to model and characterize the impact of a single particle onto a tube surface, as illustrated in Figure 1. The terminology of fluid droplet impact and the stages of a typical impact are shown in Figure 2.

Droplet impact is a complex phenomenon. To make the problem tractable, the model incorporates several assumptions:

- the particle is completely molten at the moment of impact, and contains no unburned carbon. This assumption is more valid at higher flue gas temperatures. The impact of a partially solidified particle is considered briefly near the end of this paper.
- the influence of the surrounding gas phase on the liquid phase during the few milliseconds of impact is negligible, so that only the liquid phase need be modelled. The density ratio between the liquid phase and the gas phase precludes a significant influence over such a small time. The gas phase certainly affects the particle during flight, which is reflected in the initial conditions imposed on the model (impact velocity, particle diameter, and particle composition).
- the characteristic time for fluid deformation is much smaller than for solidification, so that the effect of solidification on the final fluid configuration may be ignored.
- impact occurs normal to a smooth, solid, and flat surface. This assumption represents a limiting case, and best reflects particle impact onto a bare tube surface. The effect of surface roughness on the numerical results is presented. The assumption that the surface is solid also implies that previously deposited particles have completely solidified.

The assumptions reduce the problem to solving the equations of conservation of fluid mass and momentum within the liquid phase:

$$\nabla \cdot \vec{V} = 0 \tag{1}$$

$$\frac{\partial \vec{V}}{\partial t} + \nabla \cdot (\vec{V}\vec{V}) = -\frac{1}{\rho}\nabla p + \frac{\mu}{\rho}\nabla^2 \vec{V} + \frac{1}{\rho}\vec{F}_b \tag{2}$$

$\vec{V}$ represents velocity, p pressure, ρ density, μ viscosity and $\vec{F}_b$ any body forces acting on the fluid. Boundary conditions include the surface tension-induced pressure jump $\Delta p_s = \sigma\kappa$ across the droplet surface, where σ represents surface tension and κ the curvature of the surface, and a contact angle θ imposed at the contact line, at which the fluid surface meets the solid. Figure 3 provides an illustration.

The numerical model is a three-dimensionalization of RIPPLE, a 2D Eulerian fixed-grid fluid dynamics code developed specifically for free surface flows [1]. RIPPLE was chosen as the basis for the 3D model for two reasons: a novel approach to surface tension which was readily extended to 3D, and the capability of modelling severe fluid deformation including breakup.

Equations 1 and 2 are discretized in a control volume formulation on a rectilinear grid. Convective, viscous and surface tension effects are evaluated explicitly at each time step, followed by an implicit evaluation of pressure to enforce mass conservation. A volume tracking approach is used to track the fluid interface: a scalar function $0 \leq f \leq 1$ represents the fraction of each cell volume filled with fluid, and a geometric algorithm is used to advect f from one timestep to the next.

The 3D model differs from RIPPLE in two substantive ways. The model utilizes Youngs' 3D piecewise-linear volume tracking algorithm [2] in place of the Volume-of-Fluid algorithm of Hirt and Nichols [3] originally

implemented in RIPPLE. And the surface tension model, which treats surface tension as acting continuously on fluid near the droplet surface [4], incorporates improvements suggested by Aleinov and Puckett [5].

Grid resolution for the results presented in this paper ranged from 40 to 64 cells per initial droplet diameter, depending on the complexity of the impact. The actual grid size was considerably larger, to accommodate fluid deformation: the maximum grid size used was 192x192x64. The pressure equation was solved iteratively until the residual error decreased below 10^{-8}. Simulations were run on an SGI Indigo 2, with a typical simulation running for several days. With the exception of the most complex deformations, results changed inappreciably with further grid refinement, and are deemed to have converged. For simulations of vigorous impact and splashing behaviour (e.g. Figure 12), results continued to evolve slowly with grid refinement even on the finest grid. Such results are presented here to provide an indication of the severity of deformation.

Carryover properties were obtained by averaging values for Na_2CO_3 and Na_2SO_4 [6]: $\rho = 1900$ kg/m^3, $\mu = 5$ cP, and $\sigma = 180$ mN/m. Parameter ranges for particle size and velocity were determined from the work of Frederick and Hupa [7], who illustrate the fate of sprayed black liquor particles as a function of gas velocity and droplet diameter, and show that particles up to 2 mm in diameter may be entrained by gas velocities up to 10 m/s. Under actual boiler conditions, however, the maximum size of an entrained particle may be larger, since the flow is turbulent and highly non-uniform, with peak velocities several times the average velocity. Thus, the following parameter range was considered in this study: particle diameter from 0.1 to 3 mm; impact velocity from 3 to 10 m/s.

MODEL VALIDATION

An important part of developing a model such as this is a validation study, to assess the accuracy of the simulations against known results. To validate the model predictions, photographs were taken of carefully controlled droplet impacts, and compared with the results of corresponding simulations. Figures 4-10 illustrate the comparisons, some of which have been presented previously [8-10].

Photographs were taken of water and molten tin droplet impacts. The experimental methodology is detailed elsewhere [11,12], and is presented here only briefly. Single droplets were formed at the end of a needle, by pumping water slowly through a syringe or by applying a pressure pulse to a crucible of molten tin. The droplets detached under their own weight, and fell onto a polished stainless steel surface. A single 35 mm photograph was taken of one instant of each impact, as determined by a set time delay between droplet release and the illumination of a flash. Photographs of a particular instant during impact were sufficiently repeatable from one droplet to the next that an impact sequence could be reconstructed from photographs of different droplets.

Figure 4 shows simulation and experimental results of a 2 mm diameter water droplet impacting a 45^o inclined surface at a velocity of 1 m/s. Good qualitative agreement between photographs and simulation was obtained. From a complete set of photographs, contact angles were measured at the leading and trailing edges of the droplet. These data were then applied as a boundary condition to the simulation, with contact angles about the perimeter of the droplet interpolated linearly between the known values. A quantitative measure of the agreement is illustrated in Figure 5, where a non-dimensional spread factor ξ is defined as the ratio of instantaneous liquid-solid contact diameter to initial droplet diameter. The experimental ξ were measured from enlarged photographs; the numerical values were evaluated from simulation results.

Figure 6 illustrates the impact of a 2 mm diameter water droplet onto a 1 mm high edge at 1.2 m/s. This is an idealized geometry, but useful for validation. Rather than impose a measured variation of contact angle on this simulation, only two angles were specified, an advancing angle to an advancing contact line, and a receding angle to a receding line. Again, the comparison reveals good agreement between experiment and simulation for what is a complex impact, to the extent that the simulation accurately predicts the breakup of the droplet into two.

Figures 7-9 illustrate photographs and simulation results of the impact of 2.7 mm diameter molten tin droplets onto a flat stainless steel surface, at 1, 2 and 4 m/s respectively. The temperature of the surface was maintained just above the melting point of tin (232^oC), so that droplets remained molten after impact. A relatively constant contact angle $\theta \approx 140^o$ was measured from photographs. This value was imposed as the boundary condition at the contact line. The photographs also serve to illustrate the concepts of "fingering" and "splashing." As droplet impact becomes more vigorous, droplet spreading leads to the formation of fingers, illustrated in Figure 8. Splashing occurs when the fingers becomes unstable and pinch off.

Figure 7 demonstrates good agreement between simulation and experiment, from the initial spread of fluid to a dramatic recoil. In fact, results beyond 12 ms accurately predict fluid rebound off of the surface, and the pinch-off of a small droplet. The results of Figure 8 also agree well, although the model predicts only eight of the 14 fingers which form during the outward spread of fluid. Surprisingly, the agreement improves by 7 ms, when the 14 fingers have collapsed to eight. Finally, Figure 9 illustrates results of an impact which leads to splashing, or the formation of small satellite droplets as fingers of fluid pinch off at the perimeter of the droplet. Although agreement between simulation and experiment is more difficult to achieve, due to the fine grid resolution required to capture the formation of so many fingers at the droplet edge, the simulation nonetheless predicts the splashing behaviour, and yields a reasonable estimate of the number of satellite droplets which form.

The final validation result is presented in Figure 10, a comparison between a photograph and a corresponding simulation view of the impact of a $NaNO_3$ particle onto a smooth stainless steel surface. The photograph was taken as part of an experimental study of droplet impact using liquids analogous to carryover [13]. Note that the photograph is of a solidified droplet, a feature which is not modelled. Qualitative agreement between model and experiment is good, and the agreement extends to a reasonable prediction of the number of fingers at the droplet edge. The model predicts that fingering begins earlier than appears to have occurred experimentally. One reason for this may be the lack of a solidification model, which would act to dampen the fingering behaviour.

DISCUSSION

Effect of Contact Angle

As mentioned previously, the contact angle serves as the boundary condition to the evaluation of surface tension near the contact line, at which the fluid surface meets the solid. Figure 3 provides an illustration. The contact angle introduces to the model a quantitative measure of the wetting behaviour of the liquid on the solid surface. Quantification of such behaviour is important to understanding deposit growth: liquids which wet ($\theta \ll 90^o$) a solid will stick on impact, and fill pores between previously deposited particles; non-wetting behaviour ($\theta \gg 90^o$) leads to the possibility of fluid rebound, and to a more porous deposit.

To assess the relative importance of wetting behaviour for the range of impact conditions under consideration, simulations were run of the impact of both small and large particles, imposing different values of the contact angle. Figure 11(a) illustrates the dramatic influence of θ on the 10 m/s impact of a 0.1 mm diameter carryover particle. Impact behaviour varies from simple spreading of fluid at small contact angles to rebound of the particle from the surface for $\theta = 110^o$, as has been shown to be possible [14]. By contrast, Figure 11(b) illustrates results for the 3 m/s impact of a 3 mm diameter particle, and demonstrates that the contact angle exerts much less influence on the larger particle. The only significant difference between the two simulations occurs at the periphery of the fluid, where the larger contact angle tends to exaggerate the fingering behaviour. Otherwise, the fluid spreads to a similar extent.

This influence of contact angle versus particle size is not surprising, since surface tension varies with the curvature of a fluid surface, which increases as particle size decreases. Nevertheless, the results of Figure 11 emphasize the importance of determining a value of θ for typical carryover particle impact. The remaining simulations presented in this paper were run with $\theta = 30^o$, a wetting contact angle, for two reasons. First,

$\theta = 15^o$ was measured for a molten $NaNO_3$ droplet on a steel surface [13], which may be representative of carryover impact onto a heat transfer tube. Second, under ideal conditions (i.e. in the absence of surface contamination), a molten material wets its own solid ($\theta \approx 0^o$). The conditions within a recovery boiler are far from ideal, but since most carryover particles impact onto previously deposited ones, the choice of a relatively small value of θ is appropriate.

Effect of Particle Diameter and Velocity

Molten particle impact may be characterized by two non-dimensional quantities, the impact Reynolds number Re_o and the impact Weber number We_o, which reflect the relative magnitudes of inertial to viscous and inertial to surface tension forces respectively:

$$Re_o = \frac{\rho V_o D_o}{\mu} \quad \text{and} \quad We_o = \frac{\rho V_o^2 D_o}{\sigma} \tag{3}$$

Even the slow 1 m/s impact of a small 0.1 mm diameter carryover particle yields $Re_o \approx 40$ and $We_o \approx 1$, and these values increase rapidly as particle size and velocity increase. Thus, carryover particles are said to impact inertially, and particle size and velocity become the two most important parameters affecting impact.

Figure 12 presents an overview of the results of various simulations of carryover particle impact, for initial particle diameter $0.1 < D_o < 3$ mm and impact velocity $3 < V_o < 10$ m/s. Each entry in Figure 12 characterizes a single impact by portraying the fluid at a near-equilibrium configuration. The range over which these parameters were varied reflects the limits of particle size and velocity encountered in recovery boilers.

The most significant result is the dramatic change in impact behaviour which occurs as particle size and velocity increase. Small particles ($D_o < 0.5$ mm) spread uniformly and symmetrically, characteristic of a significant influence of surface tension. The choice of a small contact angle is evident: fluid spreads to a maximum extent, followed by little or no tendency for the fluid to recoil. Such behaviour suggests that small particles stick on impact. Also, for a given particle size, the extent of spread increases with impact velocity, as expected.

As particle size increases, the impact behaviour changes dramatically. A 1 mm diameter particle that impacts at high velocity tends to become unstable at the fluid periphery. Simulations of extremely large particles reveal that the instability leads to splashing, or the formation of small satellite droplets. At the extreme end of both the particle size and velocity ranges, a 3 mm diameter particle impacting at 10 m/s is shown to destruct into numerous smaller particles.

The onset of splashing has been related experimentally [15-17] to a critical value $\mathcal{K}_c$ of a splash parameter $\mathcal{K}$:

$$\mathcal{K} = \sqrt{We_o \sqrt{Re_o}} \propto V_o^{5/4} D_o^{3/4} \tag{4}$$

A value of $\mathcal{K}$ may be calculated for any impact from knowledge of particle size, velocity and material properties. A particle will splash when its value of $\mathcal{K}$ exceeds a critical value $\mathcal{K}_c$. Thus, for a given particle diameter, splashing occurs when impact velocity exceeds the value required to yield $\mathcal{K} > \mathcal{K}_c$, and vice versa. The simulation results of Figure 12 suggest that carryover particle impact onto a smooth surface is characterized by $\mathcal{K}_c \approx 250$, in line with other reported values [16]. However, tube surfaces, and especially existing deposits are not smooth, but rough. Cossali et al. [17] recently demonstrated that $\mathcal{K}_c$ decreases with an increase in surface roughness, and approaches an asymptotic value $\mathcal{K}_c \approx 60$ for large values of roughness.

These two values of $\mathcal{K}_c$ may be used to define the extremes of carryover particle splashing. $\mathcal{K}_c \approx 250$ is a conservative estimate of the onset of carryover splashing; $\mathcal{K}_c \approx 60$ represents an aggressive, and probably more realistic, value. Figure 13 presents both values on a plot of particle diameter versus velocity, dividing the parameter range into "splashing" (above the line) and "no splashing" regimes. Note that the location of the lines in Figure 13 corresponds to the material properties of carryover; different material properties will cause the lines to shift. The splashing regime associated with $\mathcal{K}_c = 250$ precludes the possibility that

any, but the largest particles travelling at the highest velocities will splash. The splashing regime of $\mathcal{K}_c = 60$ envelopes a much larger fraction of carryover particle impacts, and suggests that splashing may be a common outcome of the impact of particles larger than 1 mm in diameter.

These predictions of particle splashing also suggest a mechanism of formation of the very small carryover particles found in precipitator dust. The satellite particles that form as a result of splashing possess little of the forward momentum of the original particle, and instead are likely to bounce back off of the surface, to be re-entrained in the gas flow. In this way, particle impact may be thought of as a cascade, in which small particles stick to the surfaces that they impact, while the largest particles splash on impact, yielding small satellite particles which are swept further downstream.

Effect of Viscosity

Although the results presented so far have assumed a completely molten particle, this is not always the case. Depending on the flue gas temperature, particles may be molten or partially molten before impacting onto superheater tubes. The amount of liquid phase present in the particles strongly affects the particle viscosity.

In order to assess the impact of partially molten particles, the effect of viscosity was examined. Figure 14 illustrates a comparison of results of the 5 m/s impact of a 1 mm diameter carryover particle. Simulations were run for $\mu = 5$ cP, a value typical of molten carryover, and for viscosities 10 and 100 times this value. These viscosities are admittedly arbitrary, but were chosen to investigate the influence of the dramatic increase in viscosity characteristic of solidification. Clearly, as viscosity is increased viscous dissipation becomes dominant. At a viscosity 100 times the nominal value, the particle deforms only slightly from an initially spherical shape.

Finally, note that $\mathcal{K}$ decreases with an increase in viscosity, and thus inhibits splashing. Referring to Figure 13, increasing the viscosity will shift the $\mathcal{K}_c$ lines upwards and to the right.

CONCLUSIONS

A numerical model of carryover particle impact has been developed to examine the role of particle size, impact velocity and viscosity on the consequent impact behaviour. Molten carryover is assumed to wet impact surfaces; this condition was applied as a boundary condition to all simulations. Results indicate that carryover particles less than 0.5 mm in diameter are likely to impact without splashing, and to stick to tube surfaces and existing deposits, while particles greater than 1 mm in diameter will splash, forming small satellite particles that bounce from the surface and that may be re-entrained in the gas flow. This behaviour may account for the presence of the small carryover particles found in precipitator dust. Partially molten particle impact was modelled as an increase in the viscosity of the fluid; results demonstrated the influence of viscous dissipation to inhibit particle deformation.

ACKOWLEDGEMENTS

This work was part of a research program on "Control of Recovery Boiler Fireside Deposits and Corrosion," jointly supported by ABB Power Generation Segment, Ahlström Corporation, Aracruz Celulose S.A., Avenor Inc., Babcock and Wilcox Company, Boise Cascade Corporation, Clyde-Bergemann Inc., Champion International Corporation, Diamond Power International Inc., E.B. Eddy Forest Products Ltd., Fort James Corporation, Georgia Pacific Corporation, International Paper Company, Irving Pulp & Paper Ltd., Kværner Pulping Technologies, Potlatch Corporation, Union Camp Corporation, Westvaco Corporation, Weyerhaeuser Company, Willamette Industries Inc., and the Natural Sciences and Engineering Research Council of Canada.

REFERENCES

1. Kothe, D.B. and R.C. Mjolsness, RIPPLE: A new model for incompressible flows with surface tension, AIAA J., 30:2694 (1992).
2. Youngs, D.L., An interface tracking method for a 3D Eulerian hydrodynamics code, Technical Report 44/92/35, AWRE (1984).
3. Hirt, C.W. and B.D. Nichols, Volume of fluid (VOF) method for the dynamics of free boundaries, J. Comput. Phys., 39:201 (1981).
4. Brackbill, J.U., D.B. Kothe and C. Zemach, A continuum method for modeling surface tension, J. Comput. Phys., 100:335 (1992).
5. Aleinov, I. and E.G. Puckett, Computing surface tension with high-order kernels, Proceedings of the 6th International Symposium on Computational Fluid Dynamics, p.13 (1995).
6. Janz, G.J., Molten Salts Handbook, Academic Press, New York (1967).
7. Frederick, Wm.J. and M. Hupa, Black liquor droplet burning processes, Kraft Recovery Boilers, chapter 5, TAPPI Press, Atlanta (1997).
8. Bussmann, M., S. Chandra and J. Mostaghimi, Droplet impact onto arbitrary surface geometries, Proceedings of the 1997 ASME FED Summer Meeting, FEDSM97-3073.
9. Bussmann, M., S.D. Aziz, J. Mostaghimi and S. Chandra, Modelling the fingering of impacting droplets, Proceedings of CFD98, the 6th Annual Conference of the CFD Society of Canada, p.IV-43 (1998).
10. Bussmann, M., S.D. Aziz, S. Chandra and J. Mostaghimi, 3D modelling of thermal spray droplet splashing, Proceedings of the 15th International Thermal Spray Conference (1998).
11. Chandra, S. and C.T. Avedisian, On the collision of a droplet with a solid surface, Proc. R. Soc. Lond. A, 432:13 (1991).
12. Pasandideh-Fard, M., R. Bhola, S. Chandra and J. Mostaghimi, Droplet impact and solidification: Comparison of experimental and numerical results, Proceedings of the 1997 National Heat Transfer Conference, ASME HTD 347-349, p.21.
13. Mao, T., Impact of liquid droplets on solid surfaces and its application to carryover deposition in kraft recovery boilers, Ph.D. thesis, University of Toronto (1996).
14. Mao, T., D.C.S. Kuhn and H.N. Tran, Spread and rebound of liquid droplets upon impact on flat surfaces, AIChE J., 43(9):2169 (1997).
15. Stow, C.D. and M.G. Hadfield, An experimental investigation of fluid flow resulting from the impact of a water drop with an unyielding dry surface, Proc. R. Soc. Lond. A., 373:419 (1981).
16. Mundo, Chr., M. Sommerfeld and C. Tropea, Droplet-wall collisions. Experimental studies of the deformation and breakup process, Int. J. Multiphase Flow, 21(2):151 (1995).
17. Cossali, G.E., A. Coghe and M. Marengo, The impact of a single drop on a wetted solid surface, Experiments in Fluids, 22:463 (1997).

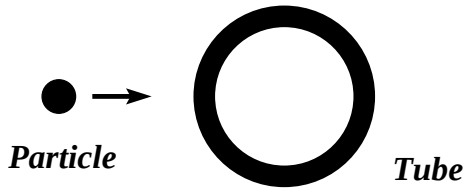

Figure 1: The impact of a single carryover particle onto a heat transfer tube (not to scale).

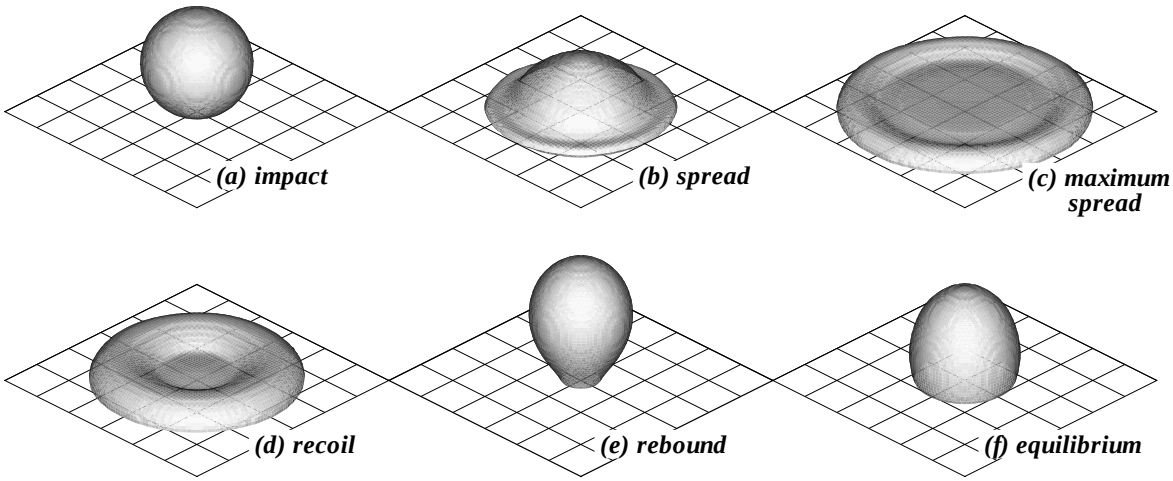

Figure 2: The stages of droplet impact: following the moment of impact (a), fluid spreads outwards (b) to a maximum extent (c). Surface tension then draws fluid back (d), possibly lifting the fluid off of the surface (e). The fluid eventually reaches an equilibrium configuration (f).

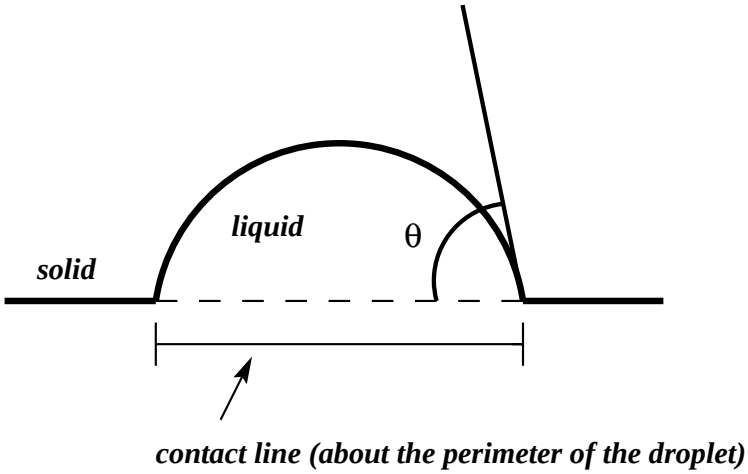

Figure 3: A two-dimensional illustration of the contact angle θ and the contact line.

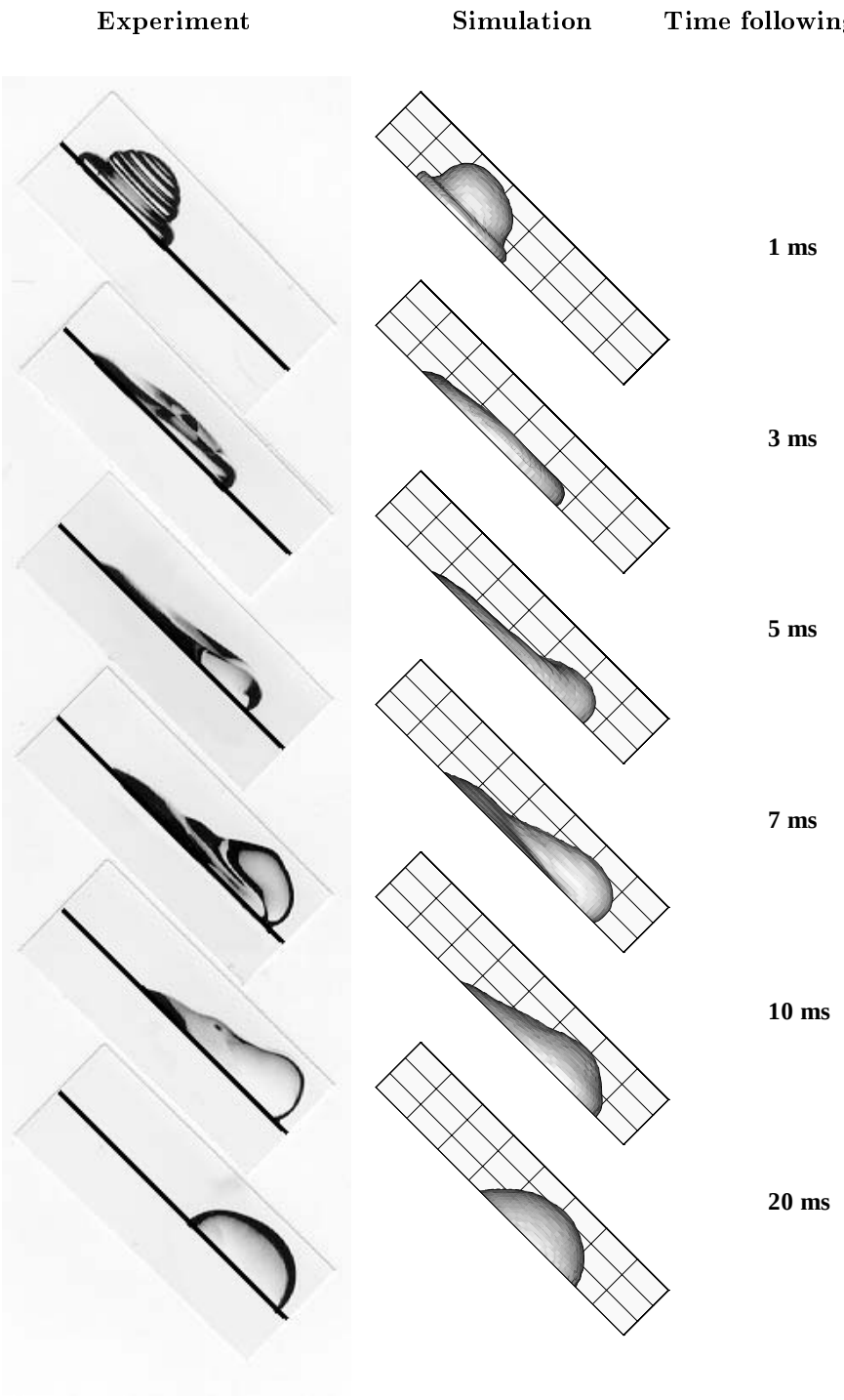

Figure 4: Profile view of the impact of a 2 mm diameter water droplet at 1 m/s onto a 45^o stainless steel incline [8]. Photographs are presented on the left; simulation results on the right. Numbers indicate time following the moment of impact.

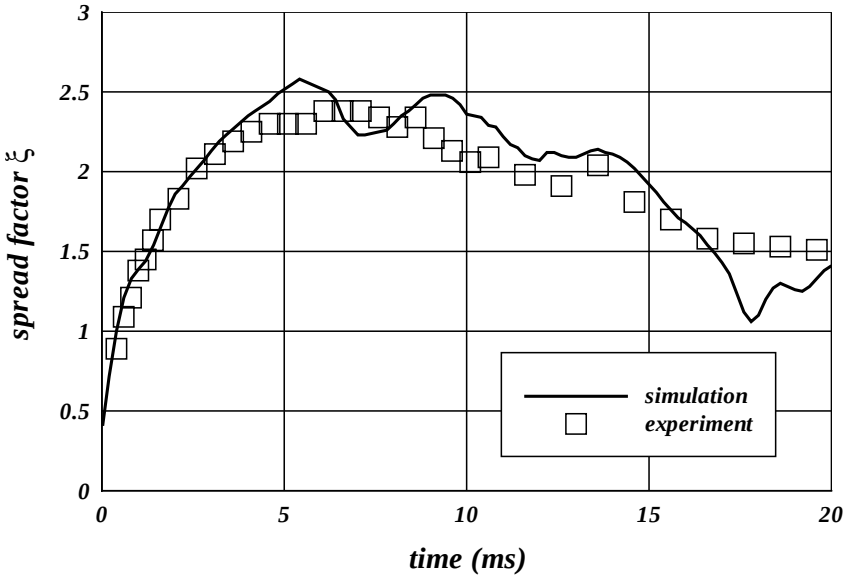

Figure 5: Spread factor ξ ($= \frac{\text{instantaneous length}}{\text{initial diameter } D_o}$) for the 45^o impact of Figure 4 [8].

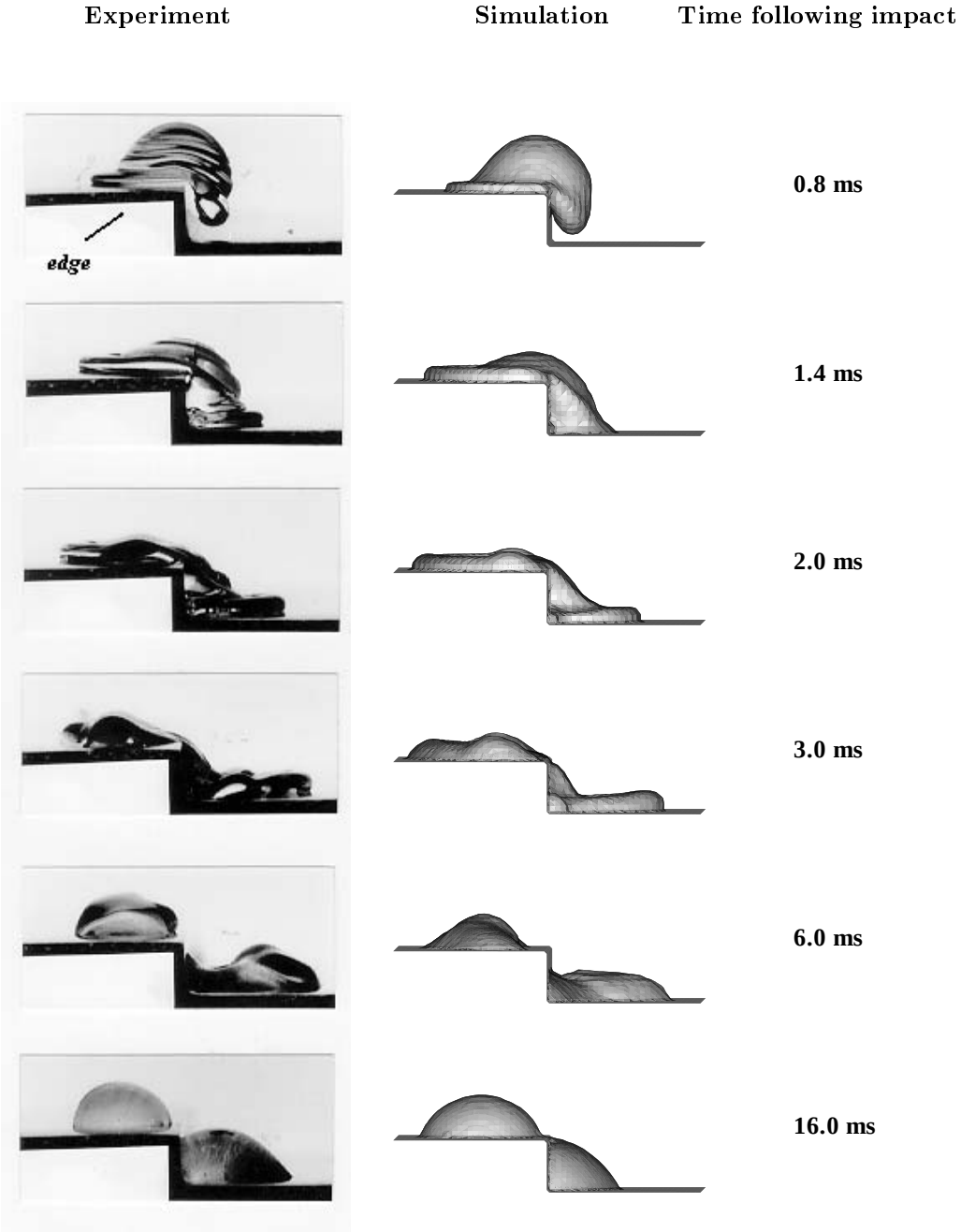

Figure 6: Profile view of the impact of a 2 mm diameter water droplet at 1.2 m/s onto a 1 mm high stainless steel edge [8]. Photographs are presented on the left, simulation results on right. Numbers indicate time following the moment of impact.

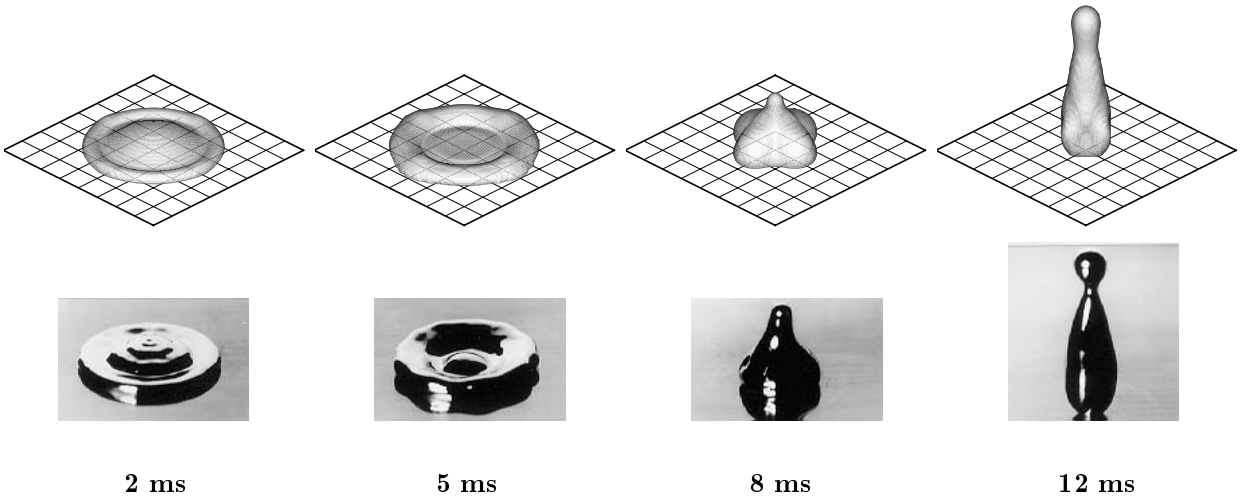

Figure 7: Simulation views and corresponding photographs of the 1 m/s impact of a 2.7 mm diameter molten tin droplet onto a hot surface [9]. Numbers indicate time following the moment of impact.

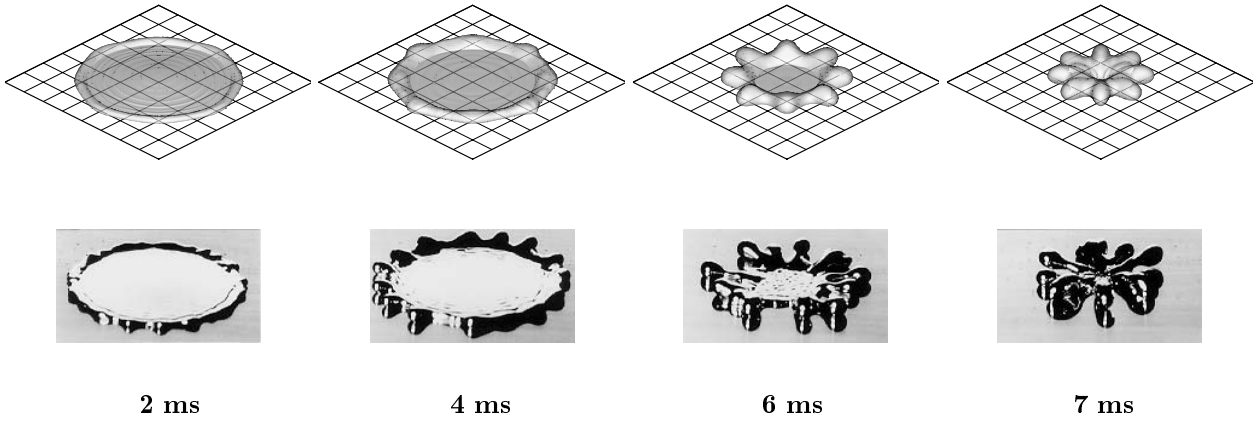

Figure 8: Simulation views and corresponding photographs of the 2 m/s impact of a 2.7 mm diameter molten tin droplet onto a hot surface [9]. Numbers indicate time following the moment of impact.

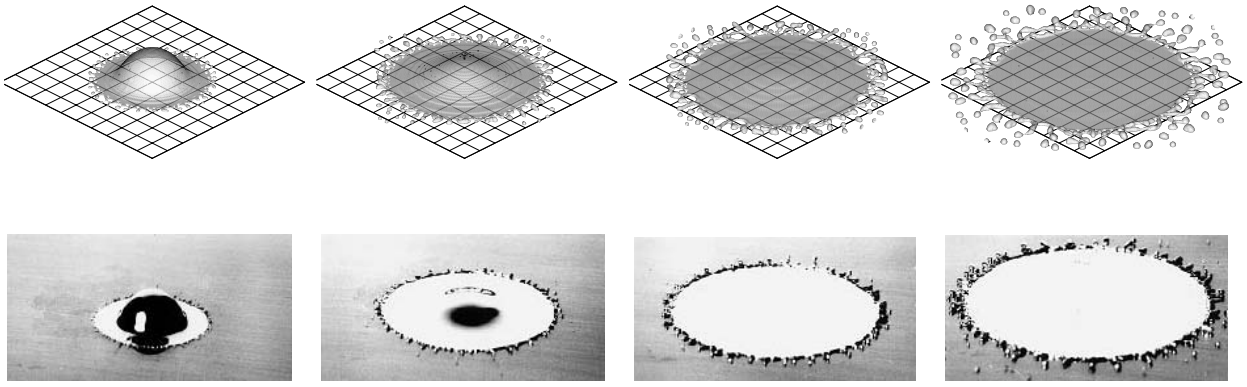

Figure 9: Simulation views and corresponding photographs of the 4 m/s impact of a 2.7 mm diameter molten tin droplet onto a hot surface [10]. Numbers indicate time following the moment of impact.

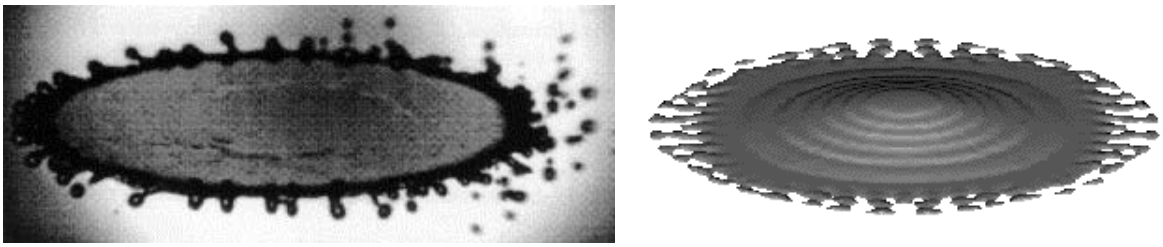

Figure 10: Photograph [13] and corresponding simulation view of the 4.2 m/s impact of a 3.1 mm diameter molten $NaNO_3$ droplet onto a cold surface. Note that the photograph is of a solidified splat, the simulation is of fluid impact only.

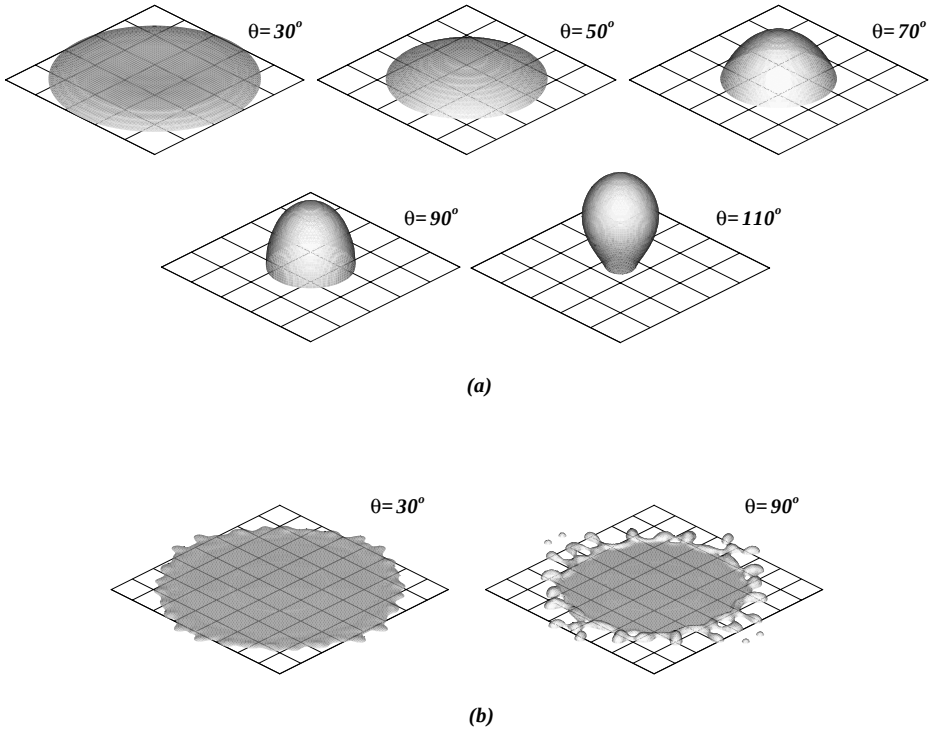

Figure 11: Influence of contact angle θ on the impact of a molten carryover particle. The illustrations are each of a different impact, corresponding to the imposed contact angle θ. (a) $D_o = 0.1$ mm, $V_o = 10$ m/s, each view at 0.125 ms after impact. (b) $D_o = 3.0$ mm, $V_o = 3$ m/s, each view at 3 ms after impact.

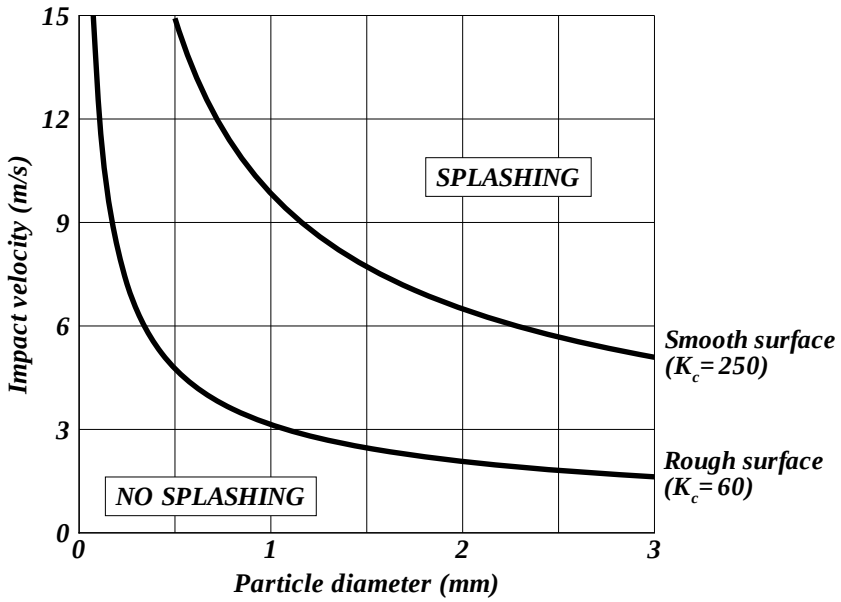

Figure 13: Splashing regime for molten carryover, for impact onto smooth and rough surfaces. The lines correspond to the following carryover properties: $\rho = 1900$ kg/m^3, $\mu = 5$ cP, and $\sigma = 180$ mN/m

.

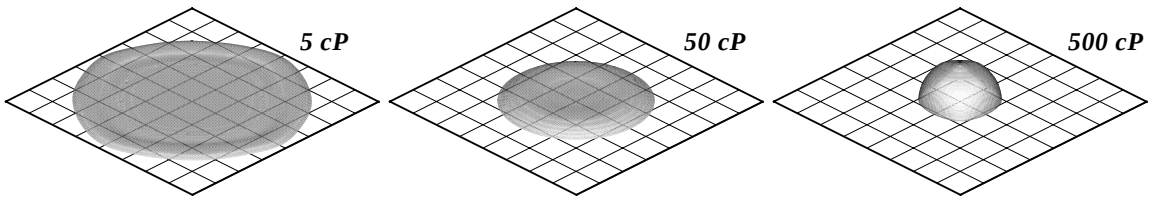

Figure 14: Influence of viscosity on the 5 m/s impact of a 1 mm diameter carryover particle. The first illustration is of the impact of a typical carryover particle; the second and third illustrations correspond to exaggerated viscosities, used to model the impact of a partially solidified particle.